

Computational study of the Sonogashira cross-coupling reaction in the gas phase and in dichloromethane solution

Lauri Sikk · Jaana Tammiku-Taul · Peeter Burk ·
András Kotschy

Received: 25 April 2011 / Accepted: 14 November 2011 / Published online: 10 December 2011
© Springer-Verlag 2011

Abstract The Sonogashira cross-coupling reaction, consisting of oxidative addition, *cis-trans* isomerization, transmetalation, and reductive elimination, was computationally modeled using the DFT B3LYP/cc-pVDZ method for reaction between bromobenzene and phenylacetylene. Palladium diphosphane was used as a catalyst, copper(I) bromide as a co-catalyst and trimethylamine as a base. The reaction mechanism was studied both in the gas phase and in dichloromethane solution using PCM method. The complete catalytic cycle is thermodynamically strongly shifted toward products (diphenylacetylene and regenerated palladium catalyst) and is exothermic being in accordance with experimental data. The rate-determining step is the oxidative addition, since the highest point on the Gibbs energy graph of the complete reaction is the transition state of this step. This conclusion is also supported by recent experimental data. The computed energy profile suggests that the transmetalation step is initiated by the dissociation of neutral ligand, while the activation Gibbs energy of this step is 0.1 kcal mol⁻¹ in the gas phase.

Keywords Cross-coupling · Density functional theory · Palladium · Sonogashira

Electronic supplementary material The online version of this article (doi:10.1007/s00894-011-1311-1) contains supplementary material, which is available to authorized users.

L. Sikk (✉) · J. Tammiku-Taul · P. Burk
Institute of Chemistry, University of Tartu,
Ravila 14A St.,
50411, Tartu, Estonia
e-mail: lsikk@ut.ee

A. Kotschy
Servier Research Institute of Medicinal Chemistry,
Záhony u. 7.,
1031, Budapest, Hungary

Introduction

The application of transition metals, especially metals in the subgroup of palladium, as catalysts in organic synthesis has become an accepted and valued tool [1–5] since the discovery of cross-coupling reactions in the first half of the 1970s. Cross-coupling reactions include numerous carbon-carbon bond forming reactions and are distinguished on the basis of the used co-catalyst or transmetalating agent. Copper is frequently used as a co-catalyst in the case of the Sonogashira coupling and conjugated acetylenes are produced from aryl halides and terminal acetylenes [2]. These fragments are often present in bioactive substances and are also important in agricultural chemistry and material science [6].

The Sonogashira cross-coupling was described for the first time in 1975 by three different groups [7–9]. The reaction mechanism (Fig. 1) consists of cycles A and B [2].

The catalytic cycle A begins with the oxidative addition of an aryl or vinyl halide or sulfonate onto a low oxidation state palladium atom, which is followed by an isomerization step. The subsequent attachment of the other coupling partner to the complex in a transmetalation step sets the stage for the final reductive elimination. Acetylenic derivative RC≡CR' is formed and the active, low oxidation state palladium catalyst is also regenerated. The catalytic cycle B describes the formation of the copper co-catalyst.

A large number of experimental data has been published for the copper co-catalyzed Sonogashira reaction [2, 10–16], but very few computational studies about the reaction mechanism can be found in the literature [14, 17]. Other palladium-catalyzed cross-coupling reactions (e.g., Heck, Stille, Suzuki reactions, etc.), which have several common steps with the Sonogashira coupling, have also been theoretically investigated [18–25].

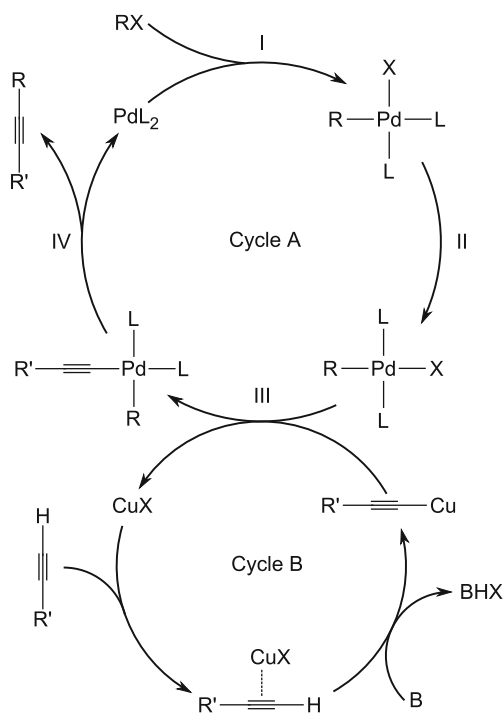


Fig. 1 Mechanism of the Sonogashira cross-coupling reaction, where I: oxidative addition; II: *cis-trans* isomerization; III: transmetalation; IV: reductive elimination

All mentioned coupling reactions start with the oxidative addition step, where the bond between carbon atom and halogen atom X breaks, while new C-Pd and X-Pd bonds are created. This is generally considered to be the rate-determining step [18]. The catalytically active palladium species is the low-ligated PdL_2 complex (L =monodentate phosphane ligand) or PdL_2X^- anion ($\text{X}=\text{Cl}, \text{Br}, \text{I}$) formed by the dissociation of stable PdL_4 catalyst. The dissociation equilibria of PdL_4 and its analogue NiL_4 have been investigated by Amatore et al. and Tsou et al. [26, 27]. The mechanism of oxidative addition is strongly dependent on the reaction conditions and can change during the course of the reaction, as the halide anion can coordinate with low-ligated palladium species and form a new active catalyst [28]. The anionic oxidative addition pathway, proposed by Amatore and Jutand [29], has been computationally investigated by Goossen et al., who concluded that the breaking of carbon-halogen bond proceeds through a pentacoordinated anionic palladium complex [22].

Mechanistic studies of the oxidative addition predict the formation of *cis*- PdL_2RX complexes, which have rarely been isolated [30, 31]. Therefore, the isomerization of *cis*- PdL_2RX to *trans*- PdL_2RX complex is proposed. Casado and Espinet have thoroughly investigated this step and found four separate pathways (two of them autocatalytic and two solvent assisted) [31]. Álvarez et al. studied these pathways computationally and concluded that the ligand-assisted mechanism was energetically the most favored [32].

The proposed role of copper co-catalyst in the Sonogashira coupling is to activate the acetylenic derivative through the formation of copper acetylide [2]. Such an activation is possible only in the presence of amines as demonstrated by Bertus et al. [33], although other bases are also used in the case of the Sonogashira coupling [34]. Reaction mechanisms for the transmetalation step describing the role of copper acetylides have also been proposed [35, 36], but no theoretical evidence can be found in the literature.

The reductive elimination step is also common for many cross-coupling reactions, similarly to the oxidative addition, and therefore, has been widely studied both experimentally [37] and theoretically [38–42]. Pérez-Rodríguez et al. demonstrated that the reductive elimination step has a number of possible reaction pathways, depending on the coordinating additives present in the reaction mixture, while the energetically most favored pathway proceeds through a four-coordinated *cis*- PdR_2L_2 complex ($\text{R}=\text{Me}, \text{Ph}, \text{vinyl}$) [41]. The steric and electronic effects of phosphane ligands can have large impact on the mechanism and rate of the reductive elimination as demonstrated by Ananikov et al. [42].

The aim of the current study was to model the Sonogashira coupling reaction in the gas phase and in solution to investigate the factors that influence the reaction rate, and to study the reaction mechanism. Understanding the uniqueness of the Sonogashira coupling might help to devise new cascade coupling processes, where selectivity is obtained through the inherent reactivity differences.

Theoretical model

The study of the Sonogashira cross-coupling reaction was carried out by determining the structures of ground states and transition states on the reaction energy hypersurface.

The Sonogashira coupling between bromobenzene, PhBr , and phenylacetylene, $\text{PhC}\equiv\text{CH}$, was modeled, where palladium diphosphane, $\text{Pd}(\text{PH}_3)_2$, was used as an active palladium catalyst, copper(I) bromide, CuBr , as a co-catalyst and trimethylamine, Me_3N , as a base. Bromobenzene, phenylacetylene, copper(I) bromide, and trimethylamine are reagents used in the synthesis of disubstituted acetylenes, while being small enough for computational study. Palladium diphosphane was chosen to represent bis(triphenylphosphane) palladium. The phosphane might be too simple a model for experimentally used bulkier triphenylphosphane and not reflect all the interactions, but we have used it to minimize computational time.

All calculations were performed using Gaussian 03 program package [43]. All geometry optimizations and vibrational analyses were done using the density functional theory (DFT) with hybrid B3LYP functional [44–47] and

the cc-pVDZ basis set [48]. In the case of copper and palladium, Stuttgart-Dresden effective core potentials with accompanying basis sets were used [49]. The gradient-corrected hybrid three-parameter B3LYP functional has been used throughout the study because previous theoretical calculations have shown that B3LYP in combination with double zeta quality basis sets and quasirelativistic energy consistent pseudopotentials of the Stuttgart-Dresden group is a cost-effective and reliable method for studying Pd- and Pt-containing systems [50, 51]. Only the lowest spin states of all species were studied. Harmonic frequency analysis was used to confirm that the found structures correspond either to minima (number of imaginary frequencies equals zero) or transition states (number of imaginary frequencies equals one). Unscaled frequencies from vibrational analysis were also used to get Gibbs energies at 1 atm and 298.15 K. Intrinsic reaction coordinate (IRC) analysis was used to verify that the obtained transition state connects reactants and products [52, 53]. Solvation Gibbs energies were calculated using polarizable continuum model (PCM) [54] by performing single point calculations for all minima and transition states (using scfvac and Radii=UFF keywords). Dichloromethane was chosen as a solvent, as it is widely used both in mechanistic studies (NMR) and synthetic procedures. Geometries and energies for all discussed structures are deposited as [Supplementary material](#).

Results and discussion

Oxidative addition

The process starts with the addition of bromobenzene to the active catalyst $\text{Pd}(\text{PH}_3)_2$ (see Fig. 2, SC) and the subsequent formation of van der Waals adduct **1** (Fig. 2). The formation of adduct **1** results in a positive Gibbs energy change ($\Delta G_{\text{GP}}=5.9 \text{ kcal mol}^{-1}$, $\Delta G_{\text{DCM}}=9.2 \text{ kcal mol}^{-1}$), which can be attributed to the loss of entropy, as the $\Delta H_{\text{GP}}=-0.1 \text{ kcal mol}^{-1}$. Structure **2** (see Fig. 2 and 3) corresponds to the transition state of oxidative addition, in which the P-Pd-P angle is 113° , the Pd-Br and Pd-C distances are 2.634 Å and 2.154 Å, respectively. The Br-C bond of bromobenzene is not coplanar with the P-Pd-P plane, probably due to the steric interaction between the phenyl group and phosphane ligands. The gas-phase Gibbs energy of transition state is $25.7 \text{ kcal mol}^{-1}$ higher than the starting compounds and solvent effects increase it to $27.9 \text{ kcal mol}^{-1}$. Oxidative addition results in the formation of planar *cis*- $\text{Pd}(\text{PH}_3)_2\text{BrPh}$ complex (**3** in Fig. 2), where the P-Pd-P angle is 103° and the Br-Pd-C angle is 89° . The Pd-P bond lengths in this complex are not equal due to the larger *trans*-effect of the phenyl group. The Pd-P bond lengths are 2.431 Å and 2.293 Å, where the longer bond corresponds to

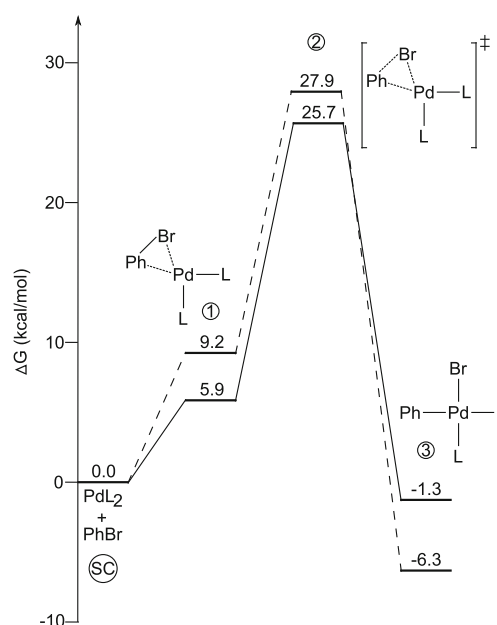


Fig. 2 Gibbs energies of the intermediate states during oxidative addition, relative to widely separated starting compounds (SC). Solid line: the gas phase; dashed line: dichloromethane (PCM); $\text{L}=\text{PH}_3$

the phosphane ligand in *trans*-position relative to the phenyl group. The formation of **3** leads to a large decrease in Gibbs energy ($\Delta G_{\text{GP}}=-1.3 \text{ kcal mol}^{-1}$, $\Delta G_{\text{DCM}}=-6.3 \text{ kcal mol}^{-1}$, relative to starting compounds).

The anionic oxidative addition reaction mechanism, proposed by Kozuch et al. [19], was investigated by coordinating bromide anion to palladium catalyst. Bromide anions, present in the reaction mixture, can interact with $\text{Pd}(\text{PH}_3)_2$, which results in the formation of complex **4** (Fig. 4). Gibbs energy of this reaction is $-14.4 \text{ kcal mol}^{-1}$ in the gas phase and $4.9 \text{ kcal mol}^{-1}$ in dichloromethane. In the subsequent formation of π -complex with bromobenzene (**5**), the bromide anion, previously coordinated to palladium, moves toward the ligands and binds to one of the hydrogen atoms of each ligand. The formation of complex **5** is highly endergonic ($16.7 \text{ kcal mol}^{-1}$ in the gas phase and $23.3 \text{ kcal mol}^{-1}$ in dichloromethane, relative to infinitely separated bromobenzene and **4**) and is accompanied by the elongation of C-Br bond in bromobenzene from 1.917 Å to 2.002 Å. Complex **6** (see Fig. 3) is the transition state of anionic oxidative addition, where the P-Pd-P angle is 99.3° . This is somewhat smaller than in the case of the neutral oxidative addition pathway (P-Pd-P 113°), which is due to the interaction of the bromide anion with the phosphane ligands. The imaginary frequency of this transition state corresponds to the C-Br bond lengthening. The gas-phase Gibbs energy of **6** relative to reactants is $10.2 \text{ kcal mol}^{-1}$, while in dichloromethane it is considerably larger ($35.7 \text{ kcal mol}^{-1}$). Complex **6** is followed by structure **7**, which after the dissociation of bromide anion, leads to *cis*- $\text{Pd}(\text{PH}_3)_2\text{BrPh}$ (**3**). The bromide

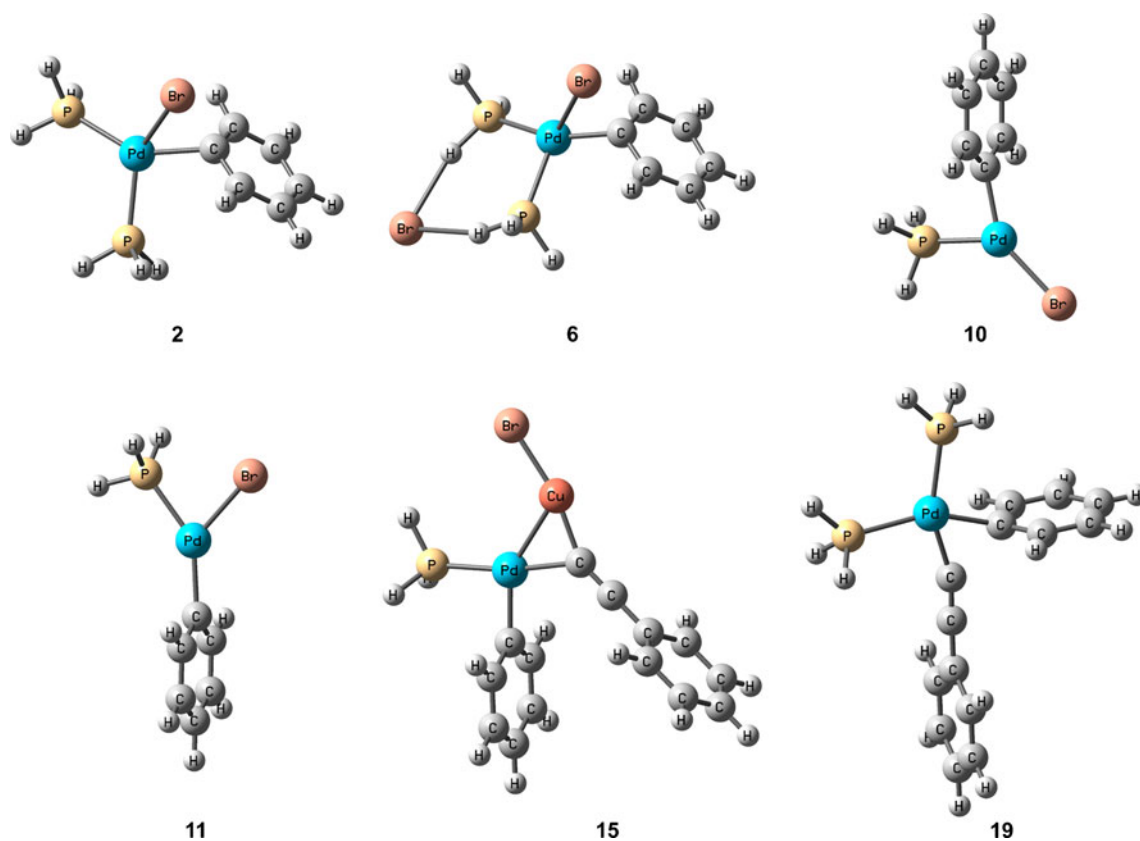


Fig. 3 Optimized structures of the transition states of the Sonogashira cross-coupling reaction

anion in **7** is bound to both ligands, causing the decrease of the P-Pd-P angle relative to complex **3** (94.7° and 103° , respectively). Therefore, the halide anion affects the oxidative addition step by interacting with the phosphane ligands and reducing the P-Pd-P angle compared to the neutral complexes. This reduced steric interaction between the ligands and bromobenzene, in turn, results in the lowering of the energy of the transition state in the gas phase (from $25.7 \text{ kcal mol}^{-1}$ to $10.2 \text{ kcal mol}^{-1}$). The situation seems to be reversed in DCM, as the transition state of anionic pathway is by $6.8 \text{ kcal mol}^{-1}$ higher, however, the used solvation model can overestimate the solvation Gibbs energy of Br^- as described by Senn et al. [55] and, severely distort the PES.

Cis-trans isomerization

Different authors have proposed numerous *cis-trans* isomerization mechanisms for coplanar Pd compounds, including isomerization through a trigonal bipyramidal transition state as a result of addition of a ligand, base or solvent molecule, as well as isomerization through a ligand dissociation [22, 31, 32]. In the present work we were unable to locate the trigonal bipyramidal transition state, so only isomerization through a dissociation of a phosphane ligand is considered.

Isomerization starts with the dissociation of one phosphane ligand. There are two ligands in the complex, thus, two reaction pathways are possible. Due to the larger *trans*-effect of the phenyl group, the phosphane ligand in *trans*-position relative to the phenyl group has weaker bonding with the Pd atom and the dissociation results in planar *cis*-Pd $(\text{PH}_3)\text{BrPh}$ complex **8** (Fig. 5).

The formation of complex **8** causes the rise in the gas-phase Gibbs energy ($4.0 \text{ kcal mol}^{-1}$), while in dichloromethane Gibbs energy of this reaction is $-1.3 \text{ kcal mol}^{-1}$. This can be attributed to solvation Gibbs energy of **8** ($\Delta G_{\text{solv}} = -6.6 \text{ kcal mol}^{-1}$), which is much larger than in the case of *cis*-Pd $(\text{PH}_3)_2\text{BrPh}$ ($\Delta G_{\text{solv}} = -1.3 \text{ kcal mol}^{-1}$). The dissociation of phosphane ligand increases the Br-Pd-C angle (from 89° to 98°), which is due to the loss of steric interaction between the phosphane ligands. Structure **10** (see Fig. 3 and 5) is the transition state of *cis-trans* isomerization proceeding through **8**, where the Br-Pd-C angle is 145° and the Pd-Br bond length has somewhat increased (from 2.416 \AA in complex **8** to 2.447 \AA in complex **10**). The relative Gibbs energy of this transition state is $8.8 \text{ kcal mol}^{-1}$ in the gas phase and $7.7 \text{ kcal mol}^{-1}$ in dichloromethane and the imaginary frequency of saddle point corresponds to the increase of Br-Pd-C angle. This transition state is followed by *trans*-Pd $(\text{PH}_3)\text{BrPh}$ complex (**12** in Fig. 5), where the Br-Pd-C angle is 162° . The end product of isomerization, *trans*-

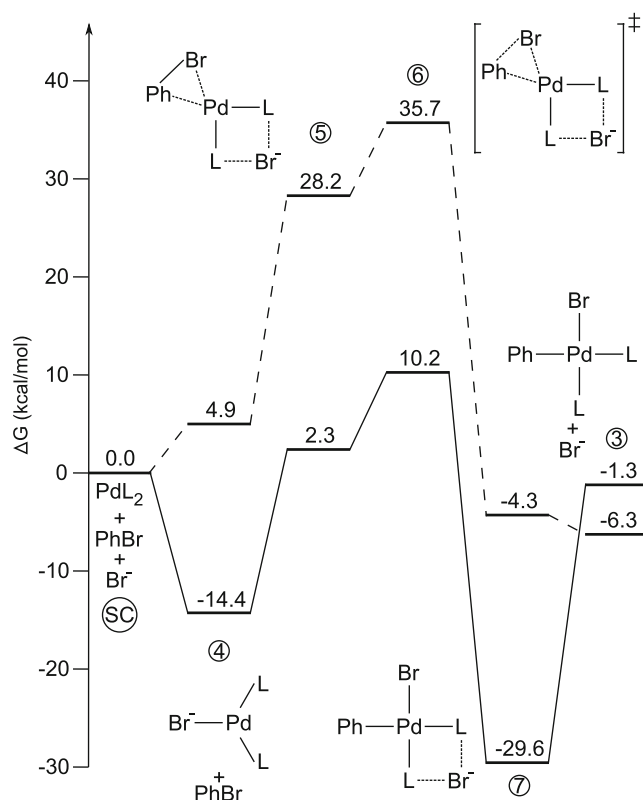


Fig. 4 Gibbs energies along the anionic oxidative addition pathway, relative to widely separated starting compounds (SC). Solid line: the gas phase; dashed line: dichloromethane (PCM); L=PH₃

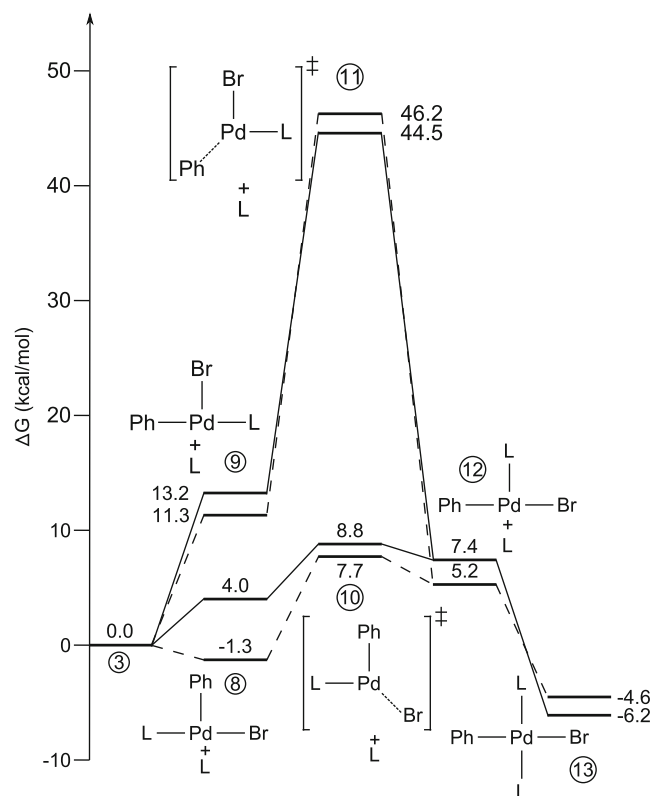


Fig. 5 Gibbs energies of *cis-trans* isomerization, relative to *cis-Pd* (PH₃)₂BrPh complex **3**. Solid line: the gas phase; dashed line: dichloromethane (PCM); L=PH₃

Pd(PH₃)₂BrPh, (**13** in Fig. 5) is formed by the addition of phosphane ligand to the complex **12**. The overall Gibbs energy change of *cis-trans* isomerization is -6.2 kcal mol⁻¹ in the gas phase and -4.6 kcal mol⁻¹ in dichloromethane.

An alternative isomerization mechanism might also be envisaged, where the phosphane ligand of Pd(PH₃)₂BrPh in *trans*-position of the bromine atom dissociates and results in the formation of complex **9** (see Fig. 5). As the bromine atom has a weaker *trans*-effect than the phenyl group, the Gibbs energy of ligand dissociation is higher ($\Delta G_{\text{GP}}=13.2$ kcal mol⁻¹, $\Delta G_{\text{DCM}}=11.3$ kcal mol⁻¹) than in the case of complex **8**. The imaginary frequency of the transition state (**11** in Fig. 3 and 5) of this alternative isomerization corresponds to the movement of phenyl group, while the Gibbs energy is much higher than the transition state of **10** ($\Delta G_{\text{GP}}=44.5$ kcal mol⁻¹, $\Delta G_{\text{DCM}}=46.2$ kcal mol⁻¹, relative to **3**, see Fig. 5).

The above described isomerization mechanisms both involve a ligand dissociation, suggesting that their rate is dependent on the concentration of free ligand (Lewis base in general). In the case of excess phosphane, the dissociation equilibrium should shift toward complex **3**, slowing down the isomerization. Urata et al. demonstrated this by using the free phosphane ligand to stop isomerization process [30].

Transmetalation and the role of copper

The proposed role of CuBr is to activate the terminal acetylenic derivative to form copper acetylide (Eq. 1). As a deprotonation process also appears, it is necessary to take into account a base (e.g., trimethylamine, Me₃N):



Gibbs energy of this reaction in the gas phase is 19.8 kcal mol⁻¹ and 8.4 kcal mol⁻¹ in dichloromethane. Phenylacetylide group is transferred from the copper atom to the Pd-complex and similarly to *cis-trans* isomerization the transmetalation step begins with the dissociation of one phosphane ligand. A possible mechanism without ligand dissociation was also investigated, but no corresponding transition state and minimum were found. The dissociation of ligand results in *trans*-Pd(PH₃)BrPh complex (**12**) and free phosphane ligand. While complex **12** is the product of *cis-trans* isomerization step, direct transmetalation reaction after isomerization is possible. On the other hand, the addition of neutral ligand (PH₃) to complex **12** results in quite large Gibbs energy drop (-13.5 kcal mol⁻¹ in the gas phase, -9.8 kcal mol⁻¹ in dichloromethane) and tetracoordinated complex **13**. Therefore, we propose that complex **13** is

present in the reaction mixture as reaction intermediate. The addition of the *trans*-complex to copper(I) phenylacetylide results in complex **14** (Fig. 6) and is accompanied by a large decrease in Gibbs energy ($-35.0 \text{ kcal mol}^{-1}$ in the gas phase and $-19.0 \text{ kcal mol}^{-1}$ in dichloromethane, relative to infinitely separated ligand, copper phenylacetylide and **12**). The Pd-Cu distance in this complex is only 2.65 \AA . Structure **15** (Fig. 3) is the transition state between complexes **14** and **16** corresponding to the decrease of C-Pd-C angle. The activation energy from complex **14** to complex **15** is very small in the gas phase ($\Delta G_{\text{act}}=0.1 \text{ kcal}$) and is negative in dichloromethane ($\Delta G_{\text{act}}=-0.7 \text{ kcal mol}^{-1}$), which can be attributed to the problems of the solvent model used. The corresponding activation electronic energies are $1.8 \text{ kcal mol}^{-1}$ and $1.2 \text{ kcal mol}^{-1}$, respectively. Structure **16** can be described as a complex between copper(I) bromide and *cis*-Pd(PH₃)(Ph)C≡CPh, as the Cu-Br bond length in **16** is close to that of free CuBr molecule (2.308 \AA and 2.210 \AA , respectively). The subsequent dissociation of copper(I) bromide and formation of complex **17** significantly increases the Gibbs energy ($37.3 \text{ kcal mol}^{-1}$ in the gas phase and $19.0 \text{ kcal mol}^{-1}$ in dichloromethane, relative to infinitely separated ligand and **16**), which can be due to the high interaction energy between the triple bond and copper atom. The addition of ligand PH₃ to complex **17** results in the product of transmetalation step (**18** in Fig. 6) with the total Gibbs energy change $4.3 \text{ kcal mol}^{-1}$ in the gas phase and $6.3 \text{ kcal mol}^{-1}$ in dichloromethane. There have recently been suggestions that amines, which are usually considered only as deprotonating agents, can also participate in oxidative addition and transmetalation steps [56]. However, the study of those mechanisms is outside the scope of the current paper.

Fig. 6 Gibbs energies of transmetalation step, relative to *trans*-Pd(PH₃)₂BrPh complex (**13**). Solid line: the gas phase; dashed line: dichloromethane (PCM); L=PH₃

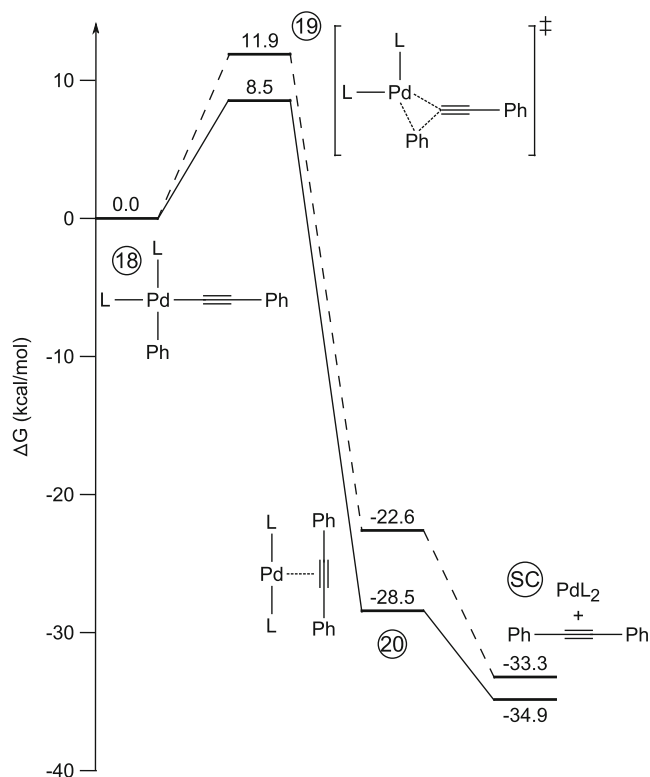
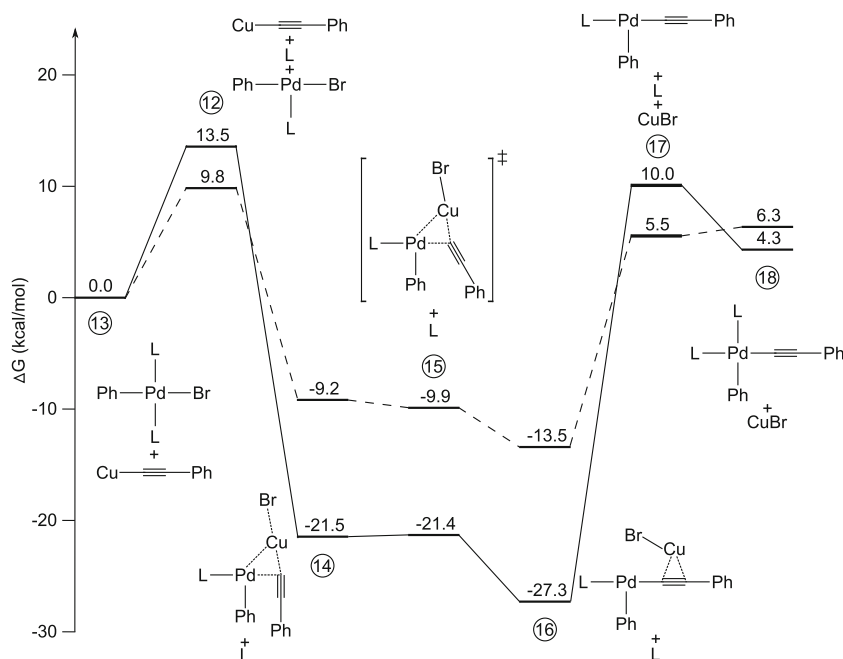


Fig. 7 Gibbs energies of reductive elimination step, relative to *cis*-Pd(PH₃)₂(Ph)C≡CPh complex (**18**). Solid line: the gas phase; dashed line: dichloromethane (PCM); L=PH₃

Reductive elimination

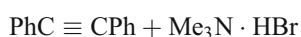
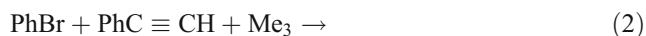
The product of the transmetalation step, *cis*-Pd(PH₃)₂(Ph)C≡CPh (**18**), decomposes into palladium diphosphane, Pd(PH₃)₂, and diphenylacetylene (tolane), Ph-C≡C-Ph, during

reductive elimination. In the transition state of the process (**19**, see Fig. 3 and 7), the C-Pd-C angle is reduced by 30° (87° → 57°) compared to the structure **18** and the distance between carbon atoms, which are bound to Pd atom, is 1.95 Å. The imaginary frequency of this transition state corresponds to the decrease of C-Pd-C angle. The activation Gibbs energy is 8.5 kcal mol⁻¹ in the gas phase and 11.9 kcal mol⁻¹ in dichloromethane.

IRC calculations for the transition state confirmed that the product of reductive elimination is complex **20**, which can be described as a complex between active catalytic species and diphenylacetylene. The subsequent dissociation of complex **20** to Pd(PH₃)₂ (**SC**) and diphenylacetylene is accompanied by further decrease in Gibbs energy (-6.4 kcal mol⁻¹ in the gas phase, -10.7 kcal mol⁻¹ in dichloromethane). This drop in Gibbs energy can be attributed to entropy, as corresponding dissociation energies are close to zero (electronic energy is 0.1 kcal mol⁻¹ in the gas phase and 0.0 kcal mol⁻¹ in dichloromethane). The overall Gibbs energy change of reductive elimination is -34.9 kcal mol⁻¹ in the gas phase and -33.3 kcal mol⁻¹ in dichloromethane.

Conclusions

Sonogashira cross-coupling is a multistep process, consisting of oxidative addition, *cis-trans* isomerization, transmetalation, and reductive elimination. The reaction mechanism was computationally studied in the presence of copper co-catalyst in the gas phase and in dichloromethane solution. The complete catalytic cycle is thermodynamically strongly shifted toward the products (see Eq. 2).



$$\Delta G_{\text{GP}} = -18.3 \text{ kcal mol}^{-1}, \Delta G_{\text{DCM}} = -28.0 \text{ kcal mol}^{-1}$$

The conclusion of our modeling is that the rate-limiting step of the process is the oxidative addition, since the highest point on the Gibbs energy graph of the complete reaction is the transition state of this addition. This prediction correlates well with recent experimental data, as the activation enthalpy of the Sonogashira cross-coupling reaction (bromobenzene and phenylacetylene in the presence of tert-Bu₃P-derived catalyst) [57] is comparable with our calculated (electronic) activation energy of the oxidative addition in the gas phase (17.7 kcal mol⁻¹ and 15.6 kcal mol⁻¹, respectively). The finding that the anionic oxidative addition is energetically favored is also in agreement with earlier experimental [58] and computational [22] results. The *cis*-geometry of the primary product of the oxidative addition,

similar to the acetate analog in [22], might rearrange to the thermodynamically more favored *trans*-complex.

The second crucial step of the catalytic cycle is the transmetalation step. Our conclusion, involving copper bromide as a co-catalyst in our model, is that, this step might be initiated by dissociation of the neutral ligand, contrary to a recent report in the literature [17]. It is important to note that the experimentally observed inhibiting effect of excess ligand on the reaction rate can be attributed to the unfavorable shift of the equilibrium in several steps, since according to our results both the *cis-trans* isomerization and the transmetalation commence by the dissociation of a ligand molecule.

Finally, we should point out the fact that copper (and palladium) might form other complexes with a number of Lewis basic entities present in the system (solvent, base, ligand, reactant, product). This suggests that computational results have to be interpreted with caution, since the specific effect of additives on the reaction path can be very strong and that fuller understanding of this fascinating and synthetically useful transformation requires the continuation of its systematic study currently ongoing in several laboratories.

Acknowledgments The authors thank the Estonian Academy of Sciences and the Hungarian Academy of Sciences for the Estonian-Hungarian Joint Research Project 2007-2009. This work was supported by Estonian Science Foundation (Grant No. 7199) and Estonian Ministry of Education and Research Targeted Financing project No. SF0180120s08. This work has been partially supported by graduate school „Functional materials and processes“ receiving funding from the European Social Fund under project 1.2.0401.09-0079 in Estonia.

References

- Kotschy A, Timári G (2005) Heterocycles from transition metal catalysis: formation and functionalization. Springer, Dordrecht
- Sonogashira KJ (2002) Development of Pd-Cu catalyzed cross-coupling of terminal acetylenes with sp²-carbon halides. *Organomet Chem* 653:46–49
- Hassan J, Sévignon M, Gozzi C, Schulz E, Lemaire M (2002) Aryl-aryl bond formation one century after the discovery of the Ullmann reaction. *Chem Rev* 102:1359–1470
- Negishi E, Anastasia L (2003) Palladium-catalyzed alkynylation. *Chem Rev* 103:1979–2017
- Zhou J, Fu GC (2004) Suzuki cross-couplings of unactivated secondary alkyl bromides and iodides. *J Am Chem Soc* 126:1340–1341
- Douchet H, Hierso JC (2007) Palladium-based catalytic systems for the synthesis of conjugated enynes by Sonogashira reactions and related alkynylations. *Angew Chem Int Edn* 46:834–871
- Diek HA, Heck FR (1975) Palladium catalyzed synthesis of aryl, heterocyclic and vinylic acetylene derivatives. *J Organomet Chem* 93:259–263
- Cassar L (1975) Synthesis of aryl- and vinyl-substituted acetylene derivatives by the use of nickel and palladium complexes. *J Organomet Chem* 93:253–257
- Sonogashira K, Tohda Y, Hagihara N (1975) A convenient synthesis of acetylenes: catalytic substitutions of acetylenic hydrogen

- with bromoalkenes, iodoarenes and bromopyridines. *Tetrahedron Lett* 16:4467–4470
- Hundertmark T, Littke AF, Buchwald SL, Fu GC (2000) Pd(PhCN)₂Cl₂/P(*t*-Bu)₃: a versatile catalyst for Sonogashira reactions of aryl bromides at room temperature. *Org Lett* 12:1729–1731
 - Pal M, Subramanian V, Yeleswarapu KR (2003) Pd/C mediated synthesis of 2-substituted benzo[b]furans/nitrobenzo[b]furans in water. *Tetrahedron Lett* 44:8221–8225
 - Li JH, Liang Y, Xie YX (2005) Efficient palladium-catalyzed homocoupling reaction and Sonogashira cross-coupling reaction of terminal alkynes under aerobic conditions. *J Org Chem* 70:4393–4396
 - Deng CL, Xie YX, Yin DL, Li JH (2006) Copper(II) acetate/1,4-diphenyl-1,4-diazabuta-1,3-diene catalyzed Sonogashira cross-coupling of aryl halides with terminal alkynes under aerobic and solvent-free conditions. *Synthesis* 20:3370–3376
 - Fairlamb IJS, O'Brien CT, Lin Z, Lam KC (2006) Regioselectivity in the Sonogashira coupling of 4,6-dichloro-2-pyrone. *Org Biomol Chem* 4:1213–1216
 - Fleckenstein CA, Plenio H (2007) 9-Fluorenylphosphines for the Pd-catalyzed Sonogashira, Suzuki, and Buchwald–Hartwig coupling reactions in organic solvents and water. *Chem Eur J* 13:2701–2716
 - Yang F, Cui X, Li Y, Zhang J, Rena G, Wua Y (2007) Cyclopalladated ferrocenylimines: efficient catalysts for homocoupling and Sonogashira reaction of terminal alkynes. *Tetrahedron* 63:1963–1969
 - Chen L, Hong S, Hou H (2008) Theoretical study on the mechanism of Sonogashira coupling reaction. *Chin J Struct Chem* 27:1404–1411
 - Lee M, Lee HM, Hu C (2007) A theoretical study of the Heck reaction: N-heterocyclic carbene versus phosphine ligands. *Organometallics* 26:1317–1324
 - Kozuch S, Amatore C, Jutand A, Shaik S (2005) What makes for a good catalytic cycle? A theoretical study of the role of an anionic palladium(0) complex in the cross-coupling of an aryl halide with an anionic nucleophile. *Organometallics* 24:2319–2330
 - Álvarez R, Faza ON, Lera AR, Cárdenas DJ (2007) A density functional theory study of the Stille cross-coupling via associative transmetalation. The role of ligands and coordinating solvents. *Adv Synth Catal* 349:887–906
 - Álvarez R, Faza ON, López CS, Lera AR (2006) Computational characterization of a complete palladium-catalyzed cross-coupling process: the associative transmetalation in the Stille reaction. *Org Lett* 8:35–38
 - Gooßen LJ, Koley D, Hermann H, Thiel W (2004) The mechanism of the oxidative addition of aryl halides to Pd-catalysts: a DFT investigation. *Chem Commun* 19:2141–2143
 - Surawatanawong P, Fan Y, Hall MB (2008) Density functional study of the complete pathway for the Heck reaction with palladium diphosphines. *J Organomet Chem* 693:1552–1563
 - Ahlquist M, Fristrup P, Tanner D, Norrby PO (2006) Theoretical evidence for low-ligated palladium(0): [Pd – L] as the active species in oxidative addition reactions. *Organometallics* 25:2066–2073
 - Ahlquist M, Norrby PO (2007) Oxidative addition of aryl chlorides to monoligated palladium (0): a DFT-SCRF study. *Organometallics* 26:550–553
 - Amatore C, Pfluger F (1990) Mechanism of oxidative addition of palladium(0) with aromatic iodides in toluene, monitored at ultramicroelectrodes. *Organometallics* 9:2276–2282
 - Tsou TT, Kochi JK (1979) Mechanism of oxidative addition. Reaction of nickel(0) complexes with aromatic halides. *J Am Chem Soc* 101:6319–6332
 - Knowles JP, Whiting A (2007) The Heck–Mizoroki cross-coupling reaction: a mechanistic perspective. *Org Biomol Chem* 5:31–44
 - Amatore C, Jutand A (2000) Anionic Pd(0) and Pd(II) intermediates in palladium-catalyzed Heck and cross-coupling reactions. *Acc Chem Res* 33:314–321
 - Urata H, Tanaka M, Fuchikami T (1987) Oxidative Addition Reaction of 1,3-Dialkyl-5-fluoro-6-iodouracils to Low-valent Transition Metal Complexes. *Chem Lett* 4:751–754
 - Casado AL, Espinet P (1998) On the configuration resulting from oxidative addition of RX to Pd(PPh₃)₄ and the mechanism of the cis-to-trans isomerization of [PdRX(PPh₃)₂] complexes (R=Aryl, X=Halide). *Organometallics* 17:954–959
 - Álvarez R, Faza ON, de Lera AR, Cárdenas DJ (2007) A density functional theory study of the Stille cross-coupling via associative transmetalation. The role of ligands and coordinating solvents. *Adv Synth Catal* 349:887–906
 - Bertus P, Fécourt F, Bauder C, Pale P (2004) Evidence for the in situ formation of copper acetylides during Pd/Cu catalyzed synthesis of enynes: a new synthesis of allenynols. *New J Chem* 28:12–14
 - Komáromi A, Tolnai GL, Novák Z (2008) Copper-free Sonogashira coupling in amine–water solvent mixtures. *Tetrahedron Lett* 49:7294–7298
 - Prokopcová H, Kappe CO (2007) Desulfitative carbon–carbon cross-coupling of thioamide fragments with boronic acids. *Adv Synth Catal* 349:448–452
 - Prokopcová H, Kappe CO (2007) Palladium(0)-catalyzed, copper (I)-mediated coupling of boronic acids with cyclic thioamides. Selective carbon-carbon bond formation for the functionalization of heterocycles. *J Org Chem* 72:4440–4448
 - Espinet P, Echavarren AM (2004) The mechanisms of the Stille reaction. *Angew Chem Int Ed* 43:4704–4732
 - Niu S, Hall MB (2000) Theoretical studies on reactions of transition-metal complexes. *Chem Rev* 100:353–405
 - Goossen LJ, Koley D, Hermann HL, Thiel W (2005) The palladium-catalyzed cross-coupling reaction of carboxylic anhydrides with arylboronic acids: a DFT study. *J Am Chem Soc* 127:11102–11114
 - Braga AC, Ujaque G, Maseras F (2006) A DFT study of the full catalytic cycle of the Suzuki – Miyaura cross-coupling on a model system. *Organometallics* 25:3647–3658
 - Peréz-Rodríguez M, Braga AC, Garcia-Melchor M, Peréz-Temprano MH, Caseras JA, Ujaque G, de Lera AR, Álvarez R, Maseras F, Espinet P (2009) C–C reductive elimination in palladium complexes, and the role of coupling additives. A DFT study supported by experiment. *J Am Chem Soc* 131:3650–3657
 - Ananikov VP, Musaev DG, Morokuma K (2007) Critical Effect of Phosphane Ligands on the Mechanism of Carbon–Carbon Bond Formation Involving Palladium(II) Complexes: A Theoretical Investigation of Reductive Elimination from Square-Planar and T-Shaped Species. *Eur J Inorg Chem* 34:5390–5399
 - Frisch MJ, Trucks GW, Schlegel HB, Scuseria GE, Robb MA, Cheeseman JR, Montgomery JA, Vreven T, Kudin KN, Burant JC, Millam JM, Iyengar SS, Tomasi J, Barone V, Mennucci B, Cossi M, Scalmani G, Rega N, Petersson GA, Nakatsuji H, Hada M, Ehara M, Toyota K, Fukuda R, Hasegawa J, Ishida M, Nakajima T, Honda Y, Kitao O, Nakai H, Klene M, Li X, Knox JE, Hratchian HP, Cross JB, Adamo C, Jaramillo J, Gomperts R, Stratmann RE, Yazyev O, Austin AJ, Cammi R, Pomelli C, Ochterski JW, Ayala PY, Morokuma K, Voth G A, Salvador P, Dannenberg JJ, Zakrzewski VG, Dapprich S, Daniels AD, Strain MC, Farkas O, Malick DK, Rabuck AD, Raghavachari K, Foresman JB, Ortiz JV, Cui Q, Baboul AG, Clifford S, Cioslowski J, Stefanov BB, Liu G, Liashenko A, Piskorz P, Komaromi I, Martin RL, Fox DJ, Keith T, Al-Laham MA, Peng CY, Nanayakkara A, Challacombe M, Gill PMW, Johnson B, Chen W, Wong MW, Gonzalez C, Pople JA (2003) Gaussian 03, Revision B.03. Gaussian Inc, Pittsburgh, PA
 - Becke AD (1993) Density-functional thermochemistry III. The role of exact exchange. *J Chem Phys* 98:5648–5652

45. Lee C, Yang W, Parr RG (1988) Development of the Colle-Salvetti correlation-energy formula into a functional of the electron density. *Phys Rev B* 37:785–798
46. Miehlich B, Savin A, Stoll H, Preuss H (1989) Results obtained with the correlation energy density functionals of Becke and Lee, Yang and Parr. *Chem Phys Lett* 157:200–206
47. Stephens PJ, Devlin FJ, Chabalowski CF, Frisch MJ (1994) Ab initio calculation of vibrational absorption and circular dichroism spectra using density functional force fields. *J Phys Chem* 98:11623–11627
48. Dunning TH (1989) Gaussian basis sets for use in correlated molecular calculations I. The atoms boron through neon and hydrogen. *J Chem Phys* 90:1007–1023
49. Schuchardt KL, Didier BT, Elsethagen T, Sun L, Gurumoorthi V, Chase J, Li J, Windus TL (2007) Basis set exchange: a community database for computational sciences. *J Chem Inf Model* 47:1045–1052
50. Beck W, Klapötke TM (2001) DFT calculations of the structures and IR frequencies of the anionic fulminate complex $[\text{Co}(\text{CNO})_6]^{3-}$, $[\text{Ni}(\text{CNO})_4]^{2-}$, $[\text{Zn}(\text{CNO})_4]^{2-}$, $[\text{Pt}(\text{CNO})_4]^{2-}$, $[\text{Au}(\text{CNO})_2]^-$ and $[\text{Hg}(\text{CNO})_4]^{2-}$. *Z Naturforsch* 56b:1376–1378
51. Beck W, Klapötke TM, Ponikvar W (2002) DFT calculations of the structures of various isomers (*cis/trans*) of $[(\text{CH}_3)(\text{PH}_3)\text{M}-\text{NH}_2-\text{CH}_2-\text{C}(\text{O})-\text{O}]$ and $[(\text{Cl})(\text{PH}_3)\text{M}-\text{NH}_2-\text{CH}_2-\text{C}(\text{O})-\text{O}]$ complexes with $\text{M} = \text{Ni}, \text{Pd}$ and Pt . *Z Naturforsch* 57b:1120–1124
52. Gonzalez C, Schlegel HB (1989) An improved algorithm for reaction path following. *J Chem Phys* 4:2154–2161
53. Gonzalez C, Schlegel HB (1991) Improved algorithms for reaction path following: higher-order implicit algorithms. *J Chem Phys* 95:5853–5860
54. Miertus S, Scrocco E, Tomasi J (1981) Electrostatic interaction of a solute with a continuum. A direct utilization of ab initio molecular potentials for the prevision of solvent effects. *Chem Phys* 55:117–129
55. Senn HM, Ziegler T (2004) Oxidative addition of aryl halides to palladium(0) complexes: a density-functional study including solvation. *Organometallics* 23:2980–2988
56. Tougerti A, Negri S, Jutand A (2007) Mechanism of the copper-free palladium-catalyzed Sonogashira reactions: multiple role of amines. *Chem Eur J* 13:666–676
57. An der Heiden MR, Plenio H, Immel S, Burello E, Rothenberg G, Hoefsloot HCJ (2008) Insights into Sonogashira cross-coupling by high-throughput kinetics and descriptor modeling. *Chem Eur J* 14:2857–2866
58. Jeffery T (1996) On the efficiency of tetraalkylammonium salts in Heck type reactions. *Tetrahedron* 52:10113–10130